Articles

Dynamic Atomic-Level Investigation of Deintercalation Processes of Mercury Titanium Disulfide Intercalates

M. McKelvy,* M. Sidorov,† A. Marie,‡ R. Sharma,† and W. Glaunsinger§,†

Center for Solid State Science, Arizona State University, Tempe, Arizona 85287-1704; Institut des Matériaux, UMR 110, University of Nantes, 44072 Nantes, France; and Department of Chemistry and Biochemistry, Arizona State University, Tempe, Arizona, 85287-1604

Received December 16, 1993. Revised Manuscript Received September 1, 1994®

Dynamic high-resolution transmission electron microscopy (DHRTEM) has been used to provide the first detailed dynamic atomic-level observations of lamellar deintercalation reaction processes. Hg_xTiS_2 ($1.25 \geq x > 0.00$) was chosen as a model low-valent (very little ionic guest–host charge transfer) intercalation system for detailed investigation. Complete deintercalation of stage-1 $Hg_{1.25}TiS_2$ was induced in situ by resistive and electron-beam heating (−170 °C to above ambient temperature). Deintercalation onset was most often observed at the externalmost guest layers, consistent with greater external host–layer flexibility. Onset also frequently occurred at internal guest layers, which can be associated with the strain induced by defects reducing the deintercalation activation energy of internal guest layers locally. Deintercalation generally progresses away from the onset layer(s) forming primarily randomly staged regions, with occasional short-range order. Guest and host–layer behavior during deintercalation provide strong support for the applicability of the Daumas–Hérold guest–island model of staging to intercalation/deintercalation reaction processes. These observations include guest–island formation and deintercalation, frequent formation of stable staggered domain-wall boundaries, and guest–layer separation. The symmetry (or asymmetry) of guest–edge dislocation terminations is directly associated with the minimization of local host–layer strain energy and host–layer restacking.

Introduction

The intercalation of lamellar host materials leads to a broad spectrum of compounds that have been of interest for decades.[1–7] Two of the most extensively investigated classes of these materials are transition-metal dichalcogenide and graphite intercalation compounds (TMDICs and GICs, respectively).[1–13] These systems are of both scientific and technological interest. A variety of unusual chemical and physical properties, including superconductivity, charge density waves, anisotropic electrical conductivity, molecular and atomic guest redox reactions, and novel structural transitions associated with the lamellar nature of the host have drawn widespread scientific attention to these materials.[1–7,11–15] Many of these intercalates have current or potential use in applications such as catalysis, low-mass electrical conductors, lubrication, and high-energy-density batteries.[1–10] Intercalation also affords unusual synthetic flexibility, including the ability to prepare a variety of derivative and intermediate compounds with compositional control.[1–7,13] This flexibility allows the tailoring of materials to have specific properties. In addition, intercalation can provide a unique low-temperature pathway to synthesize materials unattainable by conventional solid-state methods.

From a mechanistic viewpoint, TMD and graphite intercalation reactions have a formal similarity that can be described by the following reaction types: (i) ionic, (ii) redox rearrangement, and (iii) molecular.[13] The intercalation of these hosts can be classified on the basis of electron transfer, with guest-to-host electron transfer generally accompanying TMD intercalation, and both acceptor and donor electron transfer being possible for graphite intercalation due to the amphoteric nature of

† Center for Solid State Science, ASU.
‡ Institut des Matériaux
§ Department of Chemistry and Biochemistry, ASU.
® Abstract published in *Advance ACS Abstracts,* October 1, 1994.

(1) Levy, F., Ed. *Intercalated Layered Materials*; D. Reidel: Dordrecht, Holland, 1979.
(2) Whittingham, M. S., Jacobson, A. J., Eds. *Intercalation Chemistry*; Academic Press: New York, 1982.
(3) Dresselhaus, M. S., Dresselhaus, G., Fischer, J. E., Moran, M. J., Eds. *Intercalated Graphite*; North-Holland: New York, 1983.
(4) Atwood, J. L., Davies, J. E. D., MacNicol, D. D., Eds. *Inclusion Compounds*: Academic Press: London, 1984.
(5) Dresselhaus, M. S., Ed. *Intercalation in Layered Materials*; Plenum Press: New York, 1986.
(6) Legrand, A. P., Flandrois, S., Eds. *Chemical Physics of Intercalation*; Plenum Press: New York, 1987.
(7) Zabel, H., Solin, S. A., Eds. *Graphite Intercalation Compounds I*; Springer-Verlag: Berlin, 1990.
(8) Grange, P., Delmon, B. *J. Less-Common Met.* **1974**, *36*, 353.
(9) Stupian, G. W., Cosse, P. *J. Vac. Sci. Technol.* **1976**, *13*, 684.
(10) Whittingham, M. S. In *Materials Science and Energy Technology*; Libowitz, G. G., Whittingham, M. S., Eds.; Academic Press: New York, 1978; p 455.
(11) Selig, H., Ebert, L. *Adv. Inorg. Radiochem.* **1980**, *23*, 281.
(12) Forsmann, W. C.; Dziemianowicz, T.; Leong, K.; Carl, D. *Synth. Met.* **1983**, *5*, 77.
(13) McKelvy, M.; Glaunsinger W. *Annu. Rev. Phys. Chem.* **1990**, *41*, 497.
(14) Safran, S. A. *Solid State Phys.* **1987**, *40*, 183.

0897-4756/94/2806-2233$04.50/0

this host.[1−7,13] As summarized by the above reaction types, intercalation can involve (i) the formation of at least some ionic guest species during intercalation that undergo charge transfer with the host without structural rearrangement, (ii) the insertion of structurally modified, ionic guest species formed by redox reactions, and (iii) the direct insertion of the guest species into the host without the formation of ionic guest species.[13] The resulting intercalates can range in character from ionic, where only ionic guest species are present, to neutral, where the guests are essentially uncharged and can be described as experiencing at most weak covalent guest−host electron exchange.[13] The presence of either ionic or neutral guests can greatly affect guest−layer order, since electrostatic interlayer guest−guest repulsions, as opposed to host−layer elastic interactions, is believed to be the most important force associated with stage (interlayer) ordering.[15]

Staging describes the periodic arrangement of guest and host layers, with a stage-n intercalate having n host layers between nearest-neighbor guest layers. Such ordered, staged structures are generally found for intercalates that have relatively thin, flexible host layers, such as TMDICs and GICs, which enhance the electrostatic and elastic forces associated with stage ordering.[14,15] These forces are primarily derived from (i) ionic guest−host charge transfer and the resulting electrostatic interlayer repulsions and (ii) the elastic deformation of the host layers associated with the intercalation of finite-sized guests.[15,16] In addition, the host−layer separation energy, as well as individual guest−guest and guest−host interactions, must be taken into account in describing these intercalates.[15]

Integrally staged, or stage-n, intercalates have often been observed.[14−18] The interlayer forces responsible for staging can be quite long range in nature, as evidenced by the observation of stage-n intercalates up to $n = 13$ for GICs.[19] In contrast, fractionally staged, or stage n/m, intercalates have been rarely observed.[15,20−22] These materials are intermediate between stages 1 and 2 and have a periodic arrangement of m guest layers among n host layers. Although stage 3/2 and stage 4/3 GICs have been observed,[20−22] the long-range interlayer ordering forces leading to fractional staging are not well understood and may be compound specific.[15] Stage-disordered intercalates are often observed and can be stabilized either thermodynamically or kinetically.[14,15] These compounds vary substantially in their degree of stage disorder, which can range from random mixtures of different single stage-n packages (randomly staged intercalates), to complete phase (stage) separation, including all the intermediate states.[14,15,21,23−25]

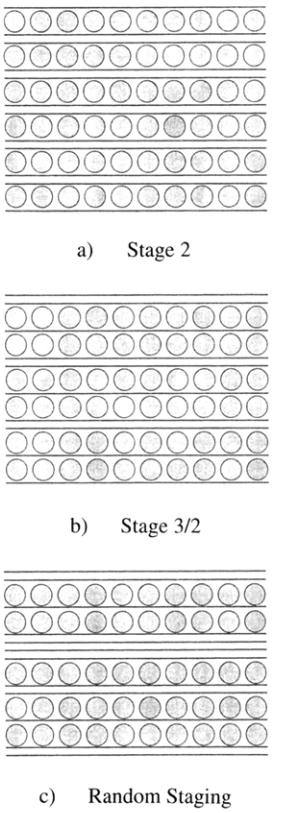

Figure 1. Classical staging model: (a) stage 2 (integral staging); (b) stage 3/2 (fractional staging); (c) random staging.

In the simple classical view, staged materials involve completely filled and empty guest galleries periodically or randomly sandwiched between host layers, as shown in Figure 1. However, substantial evidence points to the formation and intralayer motion of guest islands occurring during both intercalation and deintercalation processes,[14−17] as originally proposed by Daumas and Hérold.[26] For a stage-n compound with $n > 1$, this results in guest islands being staged locally along the c axis, with similar guest concentrations in each guest gallery, as depicted in Figure 2. Not only are intercalant island size and concentration of interest in terms of their effect on reaction processes and kinetics, they can also modify intercalate properties, including interlayer electronic conductivity and intralayer ionic conductivity.[16,27−29] Observations to date indicate guest islands can range in size from about 100 Å to macroscopic dimensions, where the intercalates approach the classical staging model.[15,16,30,31] Such classically staged materials should form in the true thermodynamic limit, where the host−layer elastic strain energy is minimized by the formation of macroscopic guest layers.[14−17] Although staging has been intensely studied theoretically and experimentally, many important issues remain unresolved, including the fundamental question of the roles of thermodynamics and kinetics in intercalation and staging processes.[14−18,25]

The Daumas−Hérold model has been widely accepted, even though studies providing experimental support

(15) Kirczenow, G. In ref 7, p 59.
(16) Ulloa, S. E., Kirczenow, G. *Comments Condens. Mater. Phys.* **1986**, *12*, 181.
(17) Safran, S. A. In ref 6, p 47.
(18) Fischer, J. E. In ref 6, p 59.
(19) Nishitani, R.; Uno, Y.; Suematsu, H. *Phys. Rev. B* **1983**, *27*, 6572.
(20) Fuerst, C. D.; Fischer, J. E.; Axe, J. D.; Hastings, J. B.; McWhan, D. B. *Phys. Rev. Lett.* **1983**, *50*, 357.
(21) Kim, H. J.; Fischer, J. E.; McWhan, D. B.; Axe, J. D. *Phys. Rev. B* **1986**, *33*, 1329.
(22) Marcus, B.; Touzain, Ph. *Synth. Met.* **1988**, *23*, 13.
(23) Kirczenow, G. *Phys. Rev. B* **1985**, *31*, 5376.
(24) Huster, M. E.; Heiney, P. A.; Cajipe, V. B.; Fischer, J. E. *Phys. Rev. B* **1987**, *35*, 3311.
(25) Cajipe, V. B.; Heiney, P. A.; Fischer, J. E. *Phys. Rev. B* **1989**, *39*, 4374.
(26) Daumas, N.; Hérold, A. *C. R. Seances Acad. Sci., Ser. C* **1969**, *268*, 373.
(27) Morelli, D. T.; Uher, C. *Phys. Rev. B* **1983**, *27*, 2477.
(28) Wiegers, G. A.; Bouwmeester, H. J. M.; Gerards, A. G. *Solid State Ionics* **1985**, *16*, 155.
(29) Bouwmeester, H. J. M. *Solid State Ionics* **1985**, *16*, 163.
(30) Timp, G.; Dresselhaus, M. S. *J. Phys. C* **1984**, *17*, 2641.
(31) Dresselhaus, M. S.; Speck, J. S. In ref 5, p 213.

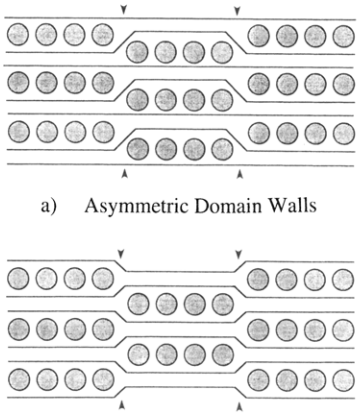

a) Asymmetric Domain Walls

b) Symmetric Domain Walls

Figure 2. Daumas–Hérold guest–island staging model: (a) stage 2 with guest–edge dislocations (GEDs) and islands forming staggered, asymmetric domain-wall boundaries; (b) stage 2 with GEDs and islands forming staggered, symmetric domain-wall boundaries. The arrows in (a) and (b) indicate the domain-wall boundary positions.

have been relatively limited in number.[14–18,32] The most direct support for this model, and staging in general, comes from atomic-level observations using high-resolution transmission electron microscopy (HRTEM). Conventional HRTEM has provided evidence for large, coherent stage-*n* regions, stage disorder ranging from random to mixed staging, and guest islands and edge dislocations.[16,30–35] Although previous observations provide insight into intercalation and staging phenomena at the atomic level, such static studies are inherently limited in the information they can provide on intercalation/deintercalation reaction processes, staging transitions, and dynamics.

Although TMDICs and GICs have been studied extensively over the past few decades, relatively little is known about their intercalation and deintercalation reaction mechanisms, especially at the atomic level. Several important issues remain unresolved regarding the associated physical processes.[15,23–25,36,37] These include how these reactions proceed, including both their onset and general progression after onset has occurred. Particular phenomena of interest whose roles during reaction progression remain unresolved include guest domain–domain interactions, sample inhomogeneities and the competition between island growth and diffusion, which can directly affect the continuous or discontinuous nature of staging transitions.[15,23,25]

Recently, we have employed environmental-cell dynamic high-resolution transmission electron microscopy (DHRTEM) to observe intercalation reaction processes at the atomic level for the first time.[38] We have also used DHRTEM to make the first atomic-level observations of staging processes associated with model ionic $Ag^{+}_{0.17}TiS_2^{0.17-}$ and neutral Hg_xTiS_2 ($1.25 \geq x > 0.00$) intercalation compounds.[39] Such dynamic studies can directly resolve reaction processes and their associated cause-and-effect relationships. Although such observations are inherently nonequilibrium in nature, they can also provide important insight into possible new-phase formation.

In this study, we report the results of a comprehensive atomic-level DHRTEM investigation of the onset and progression of deintercalation reaction processes for the model neutral intercalation system Hg_xTiS_2 ($1.25 \geq x > 0.00$).[40–43]

Experimental Section

Nearly stoichiometric TiS_2 ($Ti_{1.002\pm0.001}S_2$) was prepared by direct reaction of the elements.[44] The Hg (99.9995%) was triply distilled. Stoichiometric amounts of Hg and TiS_2 (1.25:1.00) were transferred to previously evacuated and flame-desorbed quartz ampules in a helium-containing Vacuum Atmospheres Model MO-40-1H Dri-Train glovebox (<1 ppm H_2O and O_2).[40] The reactants, under He, were then cooled to −196 °C with liquid nitrogen and evacuated to $<10^{-4}$ Torr, after which the ampules containing them were flame sealed. The reaction ampules were heated isothermally at 320 ± 2 °C for 2 days and cooled at 0.4 °C/min to ambient temperature. The resulting $Hg_{1.25}TiS_2$ was a free-flowing powder.

Mercury compositions were determined by thermogravimetric analysis (TGA) of the complete deintercalation process in an argon flow of 40 cm^3/min. The argon (99.999% Matheson Gas Products) was further purified by passing it through a R.D. Mathis GP-100 inert-gas purifier upstream from the TGA system. Samples were heated at 1 °C/min to 320 °C.

X-ray powder diffraction (XPD) was performed on a Rigaku D/Max-2B automated powder diffractometer using Cu Kα radiation. Where both Cu $K\alpha_1$ and Cu $K\alpha_2$ peaks were resolved, the Cu $K\alpha_1$ peaks were used for analysis. The diffractometer was previously standardized with NBS 640 silicon.

Samples for DHRTEM were crushed in an agate mortar and pestle under liquid nitrogen in a nitrogen cabinet.[39] XPD verified that no significant structural change occurred during crushing. The DHRTEM investigations were carried out using a JEOL 2000FX (2.5 Å point-to-point resolution) electron microscope coupled with a 30 frame/s video recording system. All of the images are taken directly from videotape (0.03 s resolution). In each image, the broad dark lines correspond to the Hg-intercalated guest galleries and the narrow dark lines correspond to the empty galleries viewed parallel to the host layers (i.e., perpendicular to the *c* axis). The crystals suitable for DHRTEM studies are inherently thin. Consequently, the crystals studied herein are limited to less than or about a few hundred angstroms in thickness parallel to the electron beam. After crushing, DHRTEM samples were transferred under nitrogen to a Gatan Model 626SP cryotransfer holder, isolated from the outside atmosphere with a cryosleeve assembly, slowly cooled to −170 °C, and loaded into the electron microscope. Initial observations of stage-1 intercalates were made at a sample holder temperature of −170 °C. The actual temperature of the crystals observed is variably higher due to some heating associated with the crystal's interaction with the electron beam. Consequently, the relevant temperatures quoted herein refer to the sample-holder temperature and not the local temperature of the crystal being observed. Hg deintercalation, as Hg(g) directly into the

(32) Hwang, D.-M. D. In ref 7, p 247.
(33) Thomas, J. M.; Millward, G. R.; Schlögl, R. F.; Boehm, H. P. *Mater. Res. Bull.* **1980**, *15*, 671.
(34) Dorignac, D.; Lahana, M. J.; Jagut, R.; Jouffrey, B.; Flandrois, S.; Hauw, C. *Mater. Res. Soc. Symp. Proc.* **1983**, *20*, 33.
(35) Matsuura, M.; Murakami, Y.; Takeda, K.; Ikeda, H.; Susuki, M. *Synth. Met.* **1985**, *12*, 427.
(36) Hooley, J. G.; Garby, W. P.; Valentin, J. *Carbon* **1965**, *3*, 7.
(37) Hooley, J. G. *Mater. Sci. Eng.* **1977**, *31*, 17; *Carbon* **1980**, *18*, 82.
(38) McKelvy, M. J.; Sharma, R.; Glausinger, W. S. *Solid State Ionics* **1993**, *63–65*, 369.
(39) McKelvy, M.; Sharma, R.; Ong, E.; Burr, G.; Glaunsinger, W. *Chem. Mater.* **1991**, *3*, 783.
(40) Ong, E. W.; McKelvy, M. J.; Ouvrard, G.; Glaunsinger, W. S. *Chem. Mater.* **1992**, *4*, 14.
(41) Moreau, P.; Ganal, P.; Ouvrard, G. *Mol. Cryst. Liq. Cryst.* **1994**, *244*, 325.
(42) Ganal, P.; Moreau, P.; Ouvrard, G.; Sidorov, M.; McKelvy, M.; Glaunsinger, W., in preparation.
(43) Sidorov, M.; McKelvy, M.; Sharma, R.; Glaunsinger, W.; Ganal, P.; Moreau, P.; Ouvrard, G., manuscript in preparation.
(44) McKelvy, M. J.; Glaunsinger, W. S. *J. Solid State Chem.* **1987**, *66*, 181.

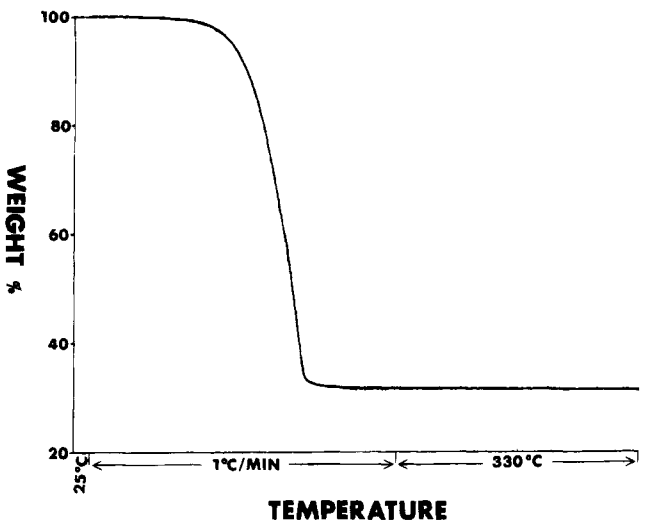

Figure 3. Thermogravimetric analysis of stage-1 $Hg_{1.25}TiS_2$. TGA of all the intercalates studied gave a consistent composition of $Hg_{1.25\pm0.01}TiS_2$.

microscope vacuum, was then induced by slow, controlled resistive heating of the sample holder together with qualitatively controlled electron-beam heating, from the initial sample temperature of −170 °C to above ambient temperature. Cooling the intercalates to −170 °C prior to loading them into the electron microscope avoids the problem of Hg deintercalation in the microscope vacuum prior to observation. Such deintercalation may be the reason for the difference in the stages previously observed by HRTEM and XPD for nominally the same sample.[32] Furthermore, vacuum deintercalation may occur at lower temperatures for microscopic TEM specimens than for bulk intercalates.[32]

Results and Discussion

Sample Characterization. XPD of the $Hg_{1.25}TiS_2$ samples was in good agreement with previous studies of $Hg_{1.25}TiS_2$, verifying that it is a single-phase, stage-1 (8.7 Å layer repeat distance) compound.[40] HRTEM observations of mercury-intercalated and empty host galleries show they generally have layer spacings of 8.7 and 5.7 Å, respectively, consistent with the layer spacings determined by XPD.

TGA of the intercalates consistently gave a composition of $Hg_{1.25\pm0.01}TiS_2$. A typical TGA curve is shown in Figure 3. For a relatively slow heating rate of 1 °C/min, 98% of the Hg deintercalated by 240 °C, and essentially all of the Hg was removed by 290 °C. This is significantly lower than the 330 °C previously reported for complete deintercalation of $Hg_{0.48}TiS_2$, which may be a result of the faster 2 °C/min TGA heating rate used in the previous study.[40,45] The higher temperature previously observed for complete deintercalation of $Hg_{0.48}TiS_2$ may also be associated with the presence of well-annealed and stable Daumas–Hérold guest islands in this stage-disordered material.[40] XPD and oxidative TGA of the regenerated host demonstrated the complete structural and compositional reversibility of the intercalation process.[40]

DHRTEM of the Deintercalation Process. *A. General Observations.* As expected for this lamellar compound, deintercalation was observed only parallel to the host layers. This result is consistent with macroscopic observations of the intercalation of highly oriented pyrolytic graphite by Hooley et al., which indicated intercalant diffusion perpendicular to the host layers was insignificant.[36,37] It is also in agreement with the inability of silver to diffuse perpendicular to the host layers during Ag_xTiS_2 intercalation.[46] While many individual guest layers deintercalated completely in a few seconds or less, others rapidly deintercalated part way only to be trapped, at least temporarily, due to host–lattice interactions.

Most often mercury deintercalation was observed to occur by formation of guest–edge dislocations (GEDs) at one side or in the middle of a crystal, followed by the movement of their terminations to the outside of the crystal, with the concurrent deintercalation of mercury.[38,39] The observation that the majority of deintercalation-related events are found progressing from left-to-right or right-to-left in the crystal, instead of from front to back, can be associated with the dimensions of the crystals that are necessary for DHRTEM observation. The crystals suitable for DHRTEM observation parallel to their layers are limited to a few hundred angstroms in thickness parallel to the electron beam. These crystals are usually much wider than they are thick. Thus, deintercalation can occur from left-to-right or right-to-left associated with a less extensive GED termination front than it can from front to back. The shorter the GED termination front is during deintercalation, the lower the guest-layer deintercalation activation energy (E_a^d) should be due to reduced elastic strain. However, partial deintercalation was also observed parallel to the electron beam, consistent with other factors, such as the termination structure of the host layers surrounding guest layers, that can affect E_a^d.

B. Onset of Deintercalation. 1. External-layer onset: The onset of deintercalation most often occurred in the externalmost guest layers, as shown in Figure 4a. The initiation of deintercalation in these guest layers is due to the greater flexibility of the adjacent external host layers, which results in the lowest deintercalation activation energy for the externalmost guest layers in compounds with good crystalline order. This atomic-level observation is similar to the progression of the intercalation process previously proposed by Hooley, which was based on macroscopic observations of bromine–graphite intercalation.[37] His observations indicated that intercalation, at least macroscopically, initially occurs between the host layers of the lamellar regions of the crystal nearest to the basal planes, with further intercalation taking place between the host layers in progressively more internal lamellar regions of the crystal. Enhanced reactivity of the region nearest the external host layers has also been observed for the Ag intercalation of TiS_2 by Auger depth profiling.[15,47] Very recent DHRTEM studies of the ammonia 2H-TaS_2 intercalation process have extended these observations to the atomic level.[38] In these experiments, the onset of intercalation was also observed to occur in the externalmost van der Waals (vdW) gaps.

2. Internal-layer onset: As discussed above, the onset of deintercalation was most often observed to occur in the externalmost guest layers. However, it was also observed to occur frequently at internal guest layers,

(45) Wendlandt, W. *Thermal Analysis*, 3rd ed.; John Wiley & Sons: New York, 1986; pp 12–17.

(46) Kaluarachchi, D.; Frindt, R. F. *Phys. Rev. B* **1983**, *28*, 3663; *Phys. Rev. B* **1985**, *31*, 3648.

(47) Kaluarachchi, D. Ph.D. Dissertation, Simon Fraser University, 1987.

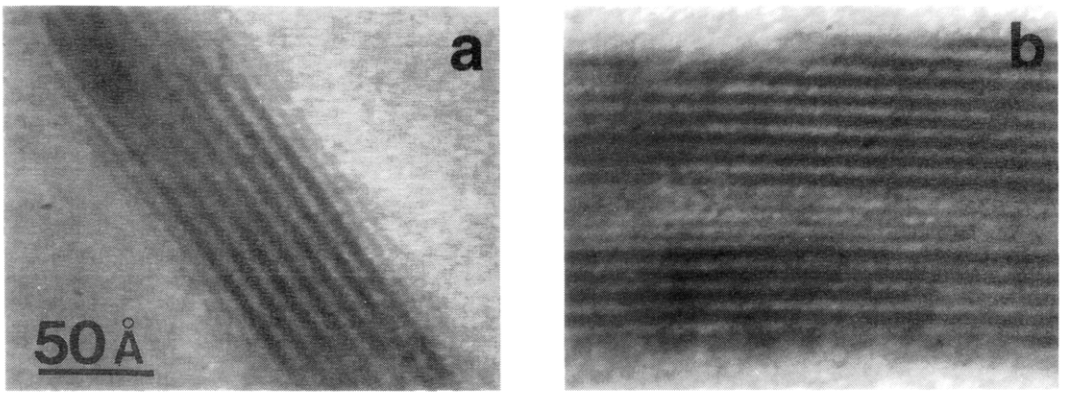

Figure 4. Deintercalation onset: (a) onset at the externalmost guest layers; (b) onset at internal guest layers.

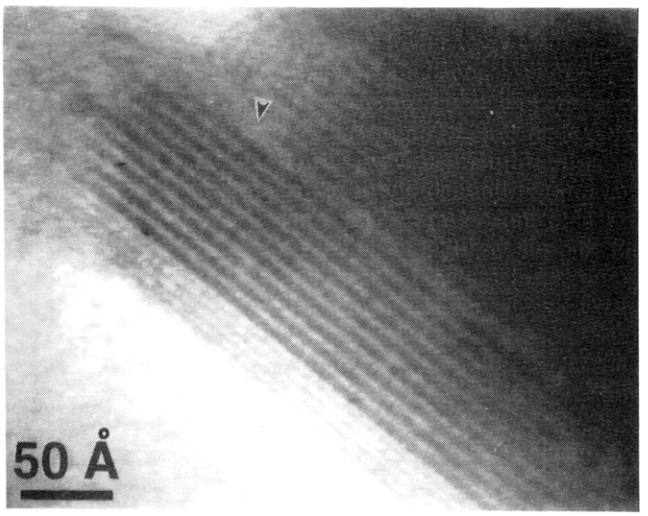

Figure 5. Simultaneous onset of deintercalation at internal and external guest layers. The arrow shows the position of the surface step associated with internal onset.

as illustrated in Figure 4b, and occasionally at both internal and external layers simultaneously, as depicted in Figure 5. The onset of deintercalation at internal guest layers can be associated with both surface and internal defects, as discussed below.

a. Surface defects: Two types of surface defects were found to be associated with the onset of internal-layer deintercalation: surface steps and irregular termination or bending of the host layers at the crystal edge. Figure 5 shows a crystal shortly after the onset of deintercalation, where the deintercalation process started at both the externalmost guest layers and an internal guest layer, whose unique feature is having its neighboring host layers terminate to form a surface step. Such internal guest layers were often observed to exhibit enhanced deintercalation reactivity.

A preference for internal-layer onset was also observed for crystals having internal guest layers whose surrounding host layers terminate irregularly at the reactive crystal edges, as shown in Figure 6. Figure 6a shows the middle of a stage-1 crystal at −170 °C prior to deintercalation. Upon warming, deintercalation started in the central layers of the crystal and then progressed to form an internal, randomly staged region surrounded by stage-1 material, as shown in Figure 6b. Careful examination of the end of the host layers at the crystal edge in Figure 6c shows irregular termination and bending of the ends of the central host layers.

The above observations provide strong evidence that surface defects can enhance the deintercalation reactivity of internal guest layers enough for initial deintercalation to occur at internal layers. For a well-ordered crystal, the activation energy needed to initiate the deintercalation process, E_a^d, should be somewhat higher for internal guest layers due to the greater rigidity of their surrounding host layers. This should lead to the onset of deintercalation in the externalmost guest layers for a well-ordered crystal. However, surface defects and/or irregularities at the edge of intercalate layers can raise or lower E_a^d. The effect on E_a^d will depend on whether the defect at the layer termination perimeter "constricts" or "expands" the host layers that surround the guest layer locally. Expansion can open the host layers and decrease E_a^d for the layer locally. In contrast, constriction can inhibit deintercalation by increasing E_a^d for guest species trying to leave through the constricted region. However, if the constriction exerts a compressive force on the guest layer locally, it may lower E_a^d for deintercalation away from the site of compression. When the guest species start to exit a layer, the host layers will collapse behind the exiting guests. This, in turn, puts more strain on the resulting guest layer at its newly formed guest−edge dislocation (GED) termination. This strain will be greater for an internal guest layer than for an outermost guest layer, due to the greater elastic strain surrounding an internal GED termination. Thus, once formed, GEDs in internal layers may exhibit enhanced deintercalation reactivity compared with those found in externalmost guest layers.

b. Internal defects: Another source of intercalate strain observed to enhance the deintercalation reactivity of internal guest layers is the presence of host−edge dislocations (HEDs), as shown in Figure 7. Figure 7a shows a stage-1 crystal containing a HED whose adjacent guest layers are fully intercalated. Upon warming, the deintercalation process starts with Hg deintercalating from the guest layer just above the HED to form a GED adjacent to the HED. The GED then moves to the lower right, as shown in Figure 7b, away from the HED termination, with deintercalation continuing until the guest layer has completely deintercalated, as illustrated in Figure 7c. In this case, the onset of deintercalation at internal guest layers partially relieves the strain induced by the HED. This is accomplished by reducing the host−layer mismatch between the layers on the right and left of the HED termination from 8.7 to 5.7 Å. It was also observed that the host layers surrounding the deintercalating guest layer move slightly further apart at the crystal edge where deintercalation is occurring. This "loosening" of guest−host bonding is a consequence of Hg diffusion and

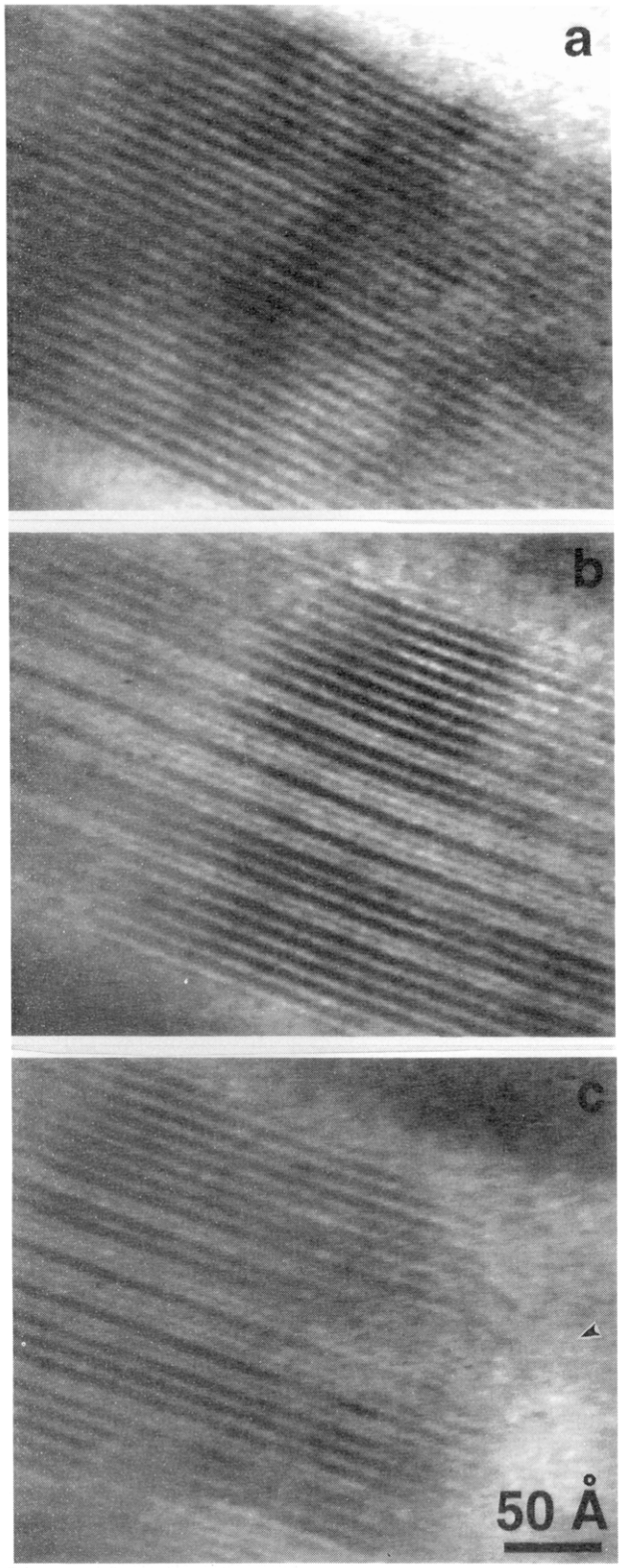

Figure 6. Internal-layer deintercalation onset associated with irregular host–layer termination at the crystal edge: (a) a stage-1 $Hg_{1.25}TiS_2$ crystal at −170 °C prior to deintercalation at; (b) the same crystal region after the onset of deintercalation in internal guest layers and after deintercalation has begun to progress away from the onset layers; (c) the right-hand termination of the same crystal at the same point in the deintercalation process shown in (b). Note the irregular termination and bending of the internal layers near the crystal edge indicated by the arrow.

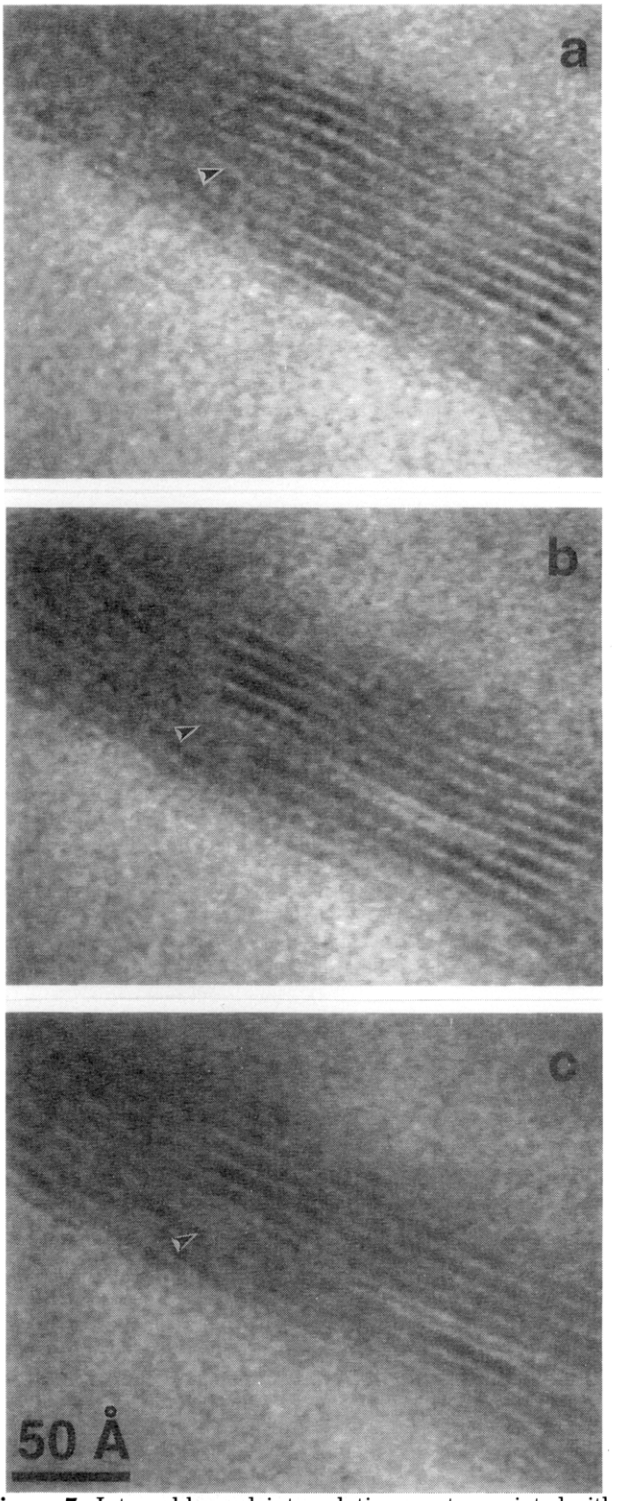

Figure 7. Internal-layer deintercalation onset associated with a host–edge dislocation (HED): (a) a stage-1 $Hg_{1.25}TiS_2$ crystal containing a HED; (b) the same region after the onset of deintercalation has begun in a guest layer adjacent to the HED, with the guest layer deintercalating together with guest–edge dislocation motion to the lower right; (c) complete deintercalation of the onset layer. The arrows show the position of the HED termination.

deintercalation, which can further lower the guest–layer E_a^d during deintercalation.

Enhanced deintercalation reactivity of internal guest layers was also observed for layers associated with interlayer defects, where nearest-neighbor host layers are displaced from their equilibrium position about the guest layer (e.g., a shear defect). Figure 8a shows a stage-1 crystal, with a region in the left part of the crystal that is defective relative to the remaining crystal. This region appears to be associated with interlayer shear, with the lower left part of the crystal bent out of the focal plane of the rest of the crystal. It could also

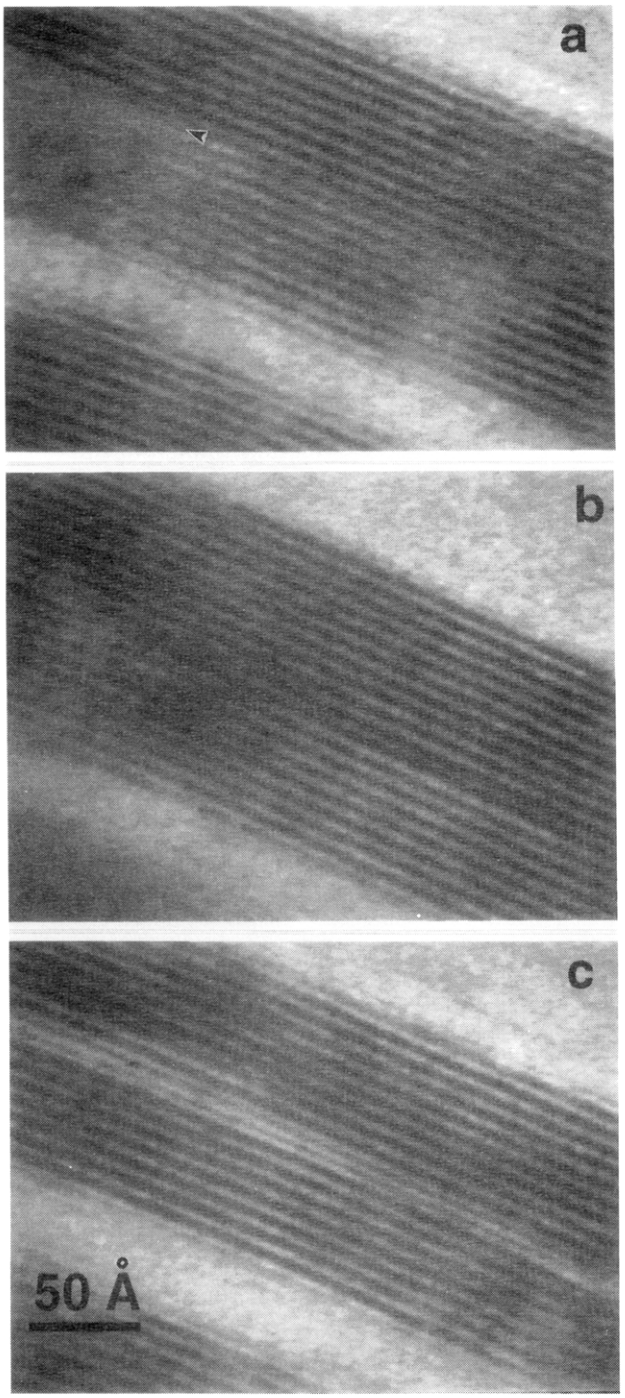

Figure 8. Internal-layer deintercalation onset associated with an interlayer defect: (a) a stage-1 $Hg_{1.25}TiS_2$ crystal containing an interlayer (probably host−layer shear) region to the left, with the defective interlayer region indicated by the arrow; (b) a region of the same crystal to the right of the interlayer defect region shown in (a) prior to deintercalation onset; (c) the same region in (b) after the onset of deintercalation.

be a region of the crystal with a significantly different thickness that is slightly tilted out of the focal plane of the rest of the crystal. In either case, the interlayer defect boundary layer is apparently under substantial strain, which can reduce its E_a^d. This defect continues to left out of the field of view in Figure 8a. The remainder of the crystal to the right is generally well formed, as shown in Figure 8b. The reduced E_a^d for the guest layer associated with the interlayer defect is confirmed by the onset of deintercalation at the interlayer−defect guest layer and a neighboring layer, as shown in Figure 8c. Thus, interlayer defects can also lead to the onset of deintercalation at internal guest layers.

C. Progression of Deintercalation. 1. After external-layer onset: Figure 9 shows the intermediate stages of the deintercalation process for a well-formed crystal. The sequence of guest−layer deintercalation is generally inward from the outermost guest layers along the *c* axis. Figure 9a shows the initial preferential deintercalation of the outer guest layers. A staggered domain wall[16] resulting from two opposing GEDs is also present in the left of Figure 9a. As the deintercalation process continues, first the outermost remaining guest layer deintercalates, as shown in Figure 9b, followed by the central layer of the stage-1 region, as illustrated in Figure 9c. This results in local stage-2 ordering of the central region of the crystal, surrounded by several deintercalated host layers. As shown in Figure 9d−f, further deintercalation proceeds from the outside in until the GED originally stabilized by a staggered domain wall in Figure 9a begins to deintercalate to the right. Together with the guest layer below it deintercalating to the left, these two GEDs form another staggered domain wall. The formation of staggered-domain walls and their behavior are discussed in more detail below.

2. After internal-layer onset: Figure 10 shows the progress of the deintercalation process after its onset for a crystal containing a host−edge dislocation. As illustrated in Figure 10a, the onset of deintercalation occurred internally and can be attributed to lattice strain relief. The two GEDs that initially formed above the HED layer during deintercalation partially compensate for the 8.7 Å interlayer mismatch between the right and left side of the crystal. Each GED reduces the mismatch by about 3 Å locally. Of particular interest is the termination of the upper GED above the HED along the *c* axis to optimally stabilize the dislocations elastically.[15,16] As deintercalation proceeds in Figure 10b, the upper GED continues to the left, as does the lower GED. The lower GED then stops just above the HED, optimally stabilizing the lower GED and HED elastically. Deintercalation next occurs for two guest layers below the HED, as shown in Figure 10c. The lower of these two layers deintercalates rapidly and completely, while the upper layer briefly pauses, with its GED terminating below the HED termination. As illustrated in Figure 10d, this GED soon deintercalates, unlike the longer-term stability observed for the GED just above the HED that persists with only slight deintercalation, as shown in Figure 10d,e. This behavior is likely due to the opposite direction of the GED above the HED, which stabilizes the GED−HED pair in a configuration similar to a staggered domain wall.[15,16] The parallel alignment of the GED below the HED depicted in Figure 10c is elastically unstable. The short-term pause of the parallel GED is probably due to a local minimization of the elastic energy associated with the unusual bending up of the layers just below the HED termination. In general, the deintercalation process then continues to move, layer by layer, away from the guest layers and the HED associated with the onset of deintercalation, as shown in Figure 10d,e.

3. General progression and staging: Once deintercalation was initiated in either the outermost or internal guest layers, further guest−layer deintercalation was qualitatively observed to follow a general pattern. First, guest layers near the onset layers would deintercalate.

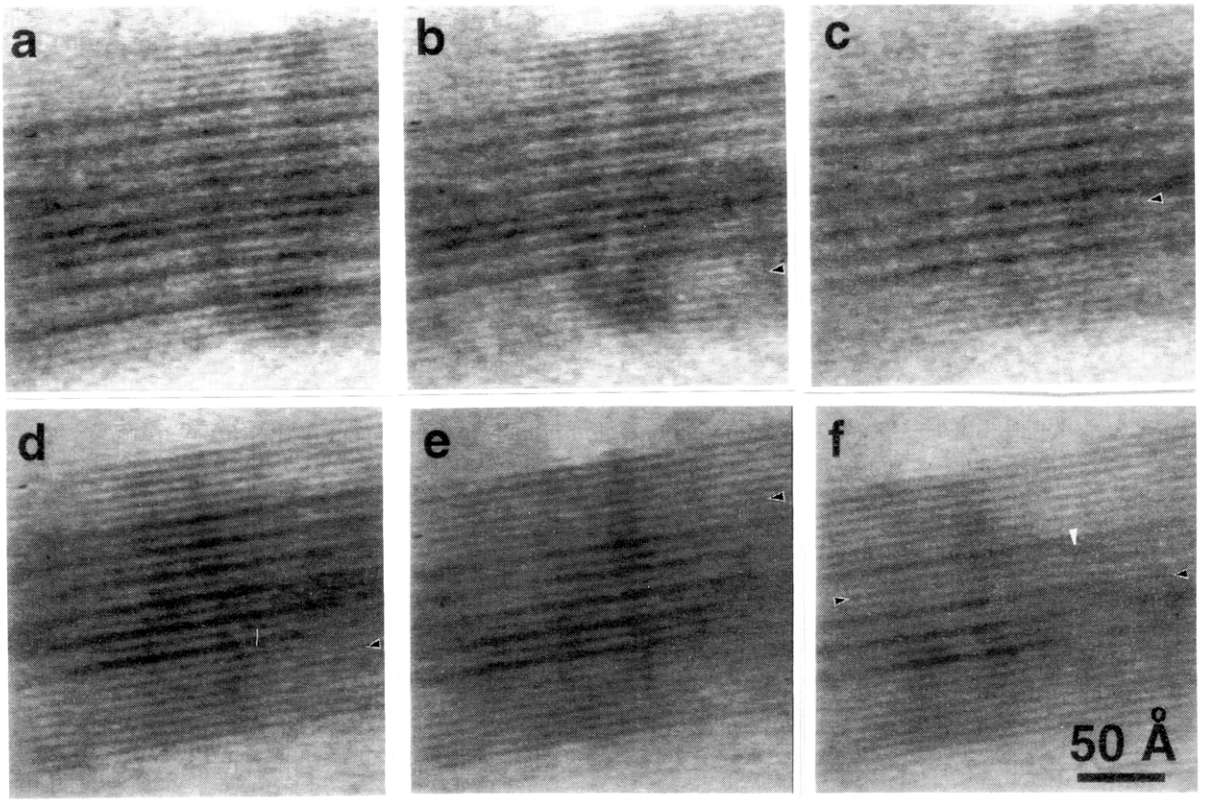

Figure 9. Typical $Hg_{1.25}TiS_2$ deintercalation progression after external onset: (a) preferential deintercalation of the outer guest layers; (b) deintercalation of the outermost remaining guest layer; (c) deintercalation of the central guest layer of the remaining stage-1 region to form an internal stage-2 region containing seven stage-2 packages; (d and e) successive deintercalation of outermost guest layers; (f) partial deintercalation of two internal guest layers to form a GED staggered domain wall indicated by the white arrow. The black on white arrows indicate the layers that have experienced deintercalation since the previous frame.

Then, as deintercalation continued, guest layers would usually deintercalate progressively further from the onset layer(s). This process generated primarily randomly staged intercalate regions, with occasional local stage ordering, expanding away from the onset layer(s). These observations indicate that once the first guest layer has deintercalated from a region, the remaining guest layers nearby become more susceptible to deintercalation.

The overall progression of the deintercalation process away from its onset layer(s) highlights the complex balance of forces that affects the $Hg_{1.25}TiS_2$ deintercalation process and may be associated with several contributing factors. Defects that lower the E_a^d of the onset guest layer(s) often lower the E_a^d of nearby layers as well. Similarly, the onset of deintercalation in the outermost guest layers is aided by the greater flexibility of the neighboring external host layers. This flexibility progressively decreases the further the guest layers are from the lamellar crystal surface, supporting the progressively deeper deintercalation of guest layers near the intercalate surface.

Other factors independent of the onset layer's proximity to an external host layer or host–lattice defect(s) can also contribute to the destabilization of guest layers near the onset layer and promote progressive deintercalation away from the onset layer. For example, the slight in-plane, host–layer mismatch between deintercalated host layers and neighboring intercalate layers (about 0.0–0.3%, as a function of the in-plane direction for the stage-1 intercalate and TiS_2)[40,42,43] will serve to destabilize the adjacent guest layers.[14,15] This promotes the deintercalation of guest layers neighboring empty guest galleries. In contrast, the interlayer repulsive forces that lead to stage ordering should promote the ordered periodic deintercalation of the guest layers.[14–18,21,23–25] Thus, the overall trend for progressive deintercalation of guest layers away from the onset layer creating stage-disordered, primarily randomly staged, regions with some local ordering clearly indicates no dominant force is governing the process. This is expected to be the case for the nonequilibrium observation of the deintercalation of neutral intercalates, such as Hg_xTiS_2. Not only does the nonequilibrium nature of the process contribute to the observed random staging, the essential absence of ionic guests also results in a lack of interlayer electrostatic repulsions that are believed to be the dominant force associated with stage ordering.[14,15] Furthermore, elastic interactions associated with Daumas–Hérold domains should not significantly affect the staging processes observed in these studies, since the relatively small crystals observed cannot support sufficient domain formation.[14–18,26] Similar stage disorder has been observed by X-ray diffraction under near equilibrium conditions for Cs-GICs, which exhibit appreciable guest–host charge transfer and guest ionic character. However, it only occurs at a relatively high average stage index, n' (i.e., at or above $n' \sim 5$ for Cs-GICs),[25] where electrostatic and interlayer repulsions in general are much weaker due to the greater distance between guest layers.

The longest-range ordered region observed for a partially deintercalated crystal contained seven stage-2 packages sandwiched between deintercalated host layers, as illustrated in Figure 9c. Shorter range ordered regions of other stages were also observed during deintercalation. A region containing four stage-3 packages was observed near the end of one deinterca-

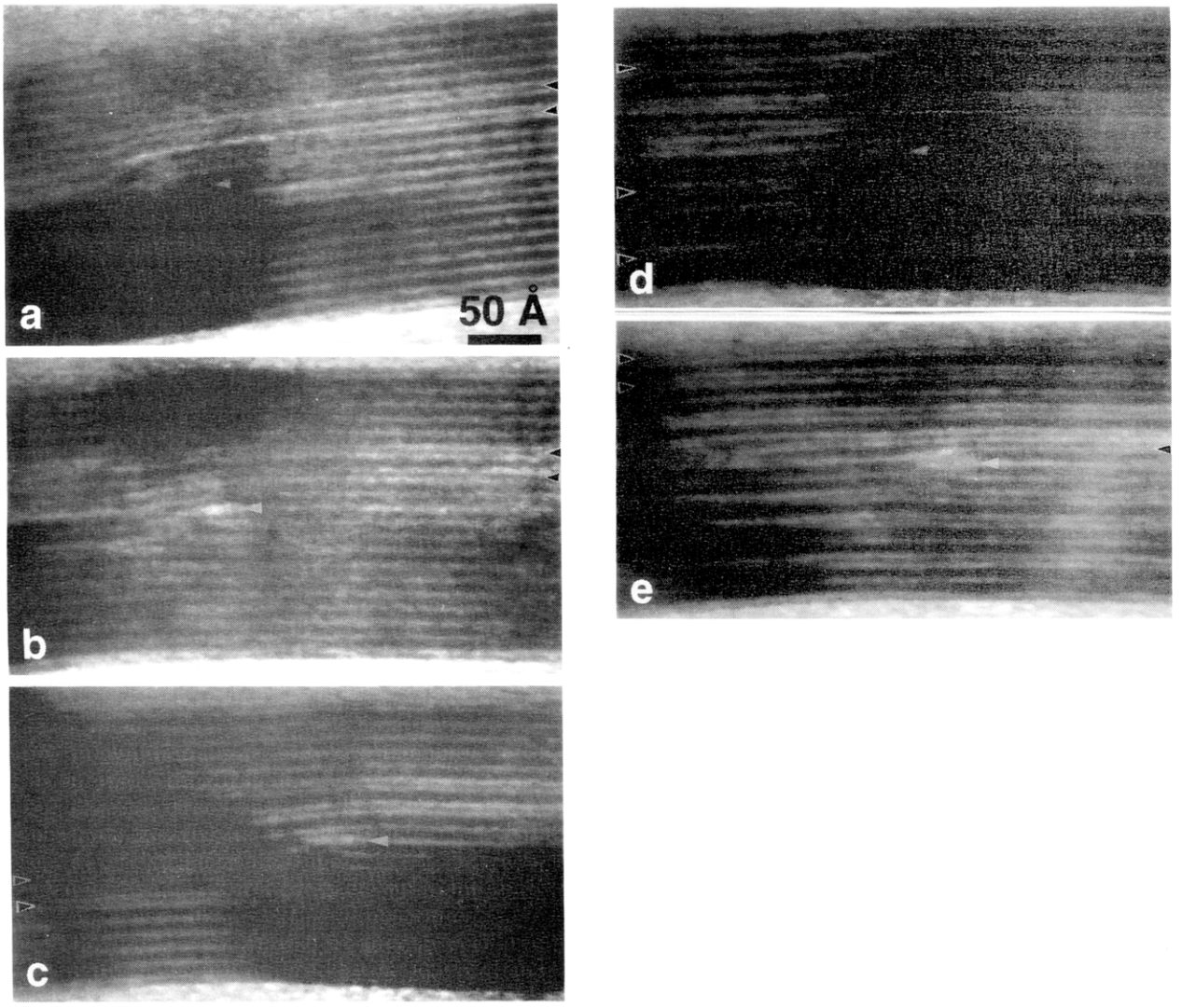

Figure 10. Typical $Hg_{1.25}TiS_2$ deintercalation progression after internal onset: (a) internal onset of deintercalation via GED formation and movement of two guest layers above the HED; (b) continued deintercalation of the upper GED-containing guest layers to the left; (c) subsequent deintercalation of guest layers below the HED; (d and e) continued deintercalation away from the HED. Note the two regions containing two stage-3/2 packages formed during deintercalation; one is near the bottom and the other is in the upper left of the crystal in (d). The white arrows indicate the position of the HED termination. The black-on-white arrows indicate the layers that have experienced deintercalation since the previous frame.

lation process (section D.2). Also, on several occasions, regions containing two and three packages of the fractional stage-3/2 were observed. Figure 10d shows the formation of two regions containing two stage-3/2 packages during deintercalation: one at the bottom of the crystal and the other at the left of the top of the crystal. These short-range ordered regions were observed under nonequilibrium conditions and, as a result, cannot be considered as representitive of true equilibrium phases. However, they do suggest such stage-ordered phases may exist. This possibility is currently under investigation.

D. Guest and Host–Layer Behavior during Deintercalation. 1. Guest–layer separation and island formation: Deintercalation was occasionally observed to start with the guest species moving away from the middle of a guest layer, as shown in Figure 11. Figure 11a shows a crystal that has started to deintercalate from the outermost guest layer in, with the uppermost remaining guest layer still intact. This guest layer then begins to separate in the middle, as Hg deintercalates, as shown in Figure 11b. This separation not only results in the formation of two GEDs, it also forms a guest island having dimensions of ≈70 Å in the process. As the separation process continues, the GEDs begin to migrate to the left and right, with the guest island shrinking to approximately 40 Å across in Figure 11c. The shrinking of the guest island suggests that it is deintercalating parallel to the electron beam, since no movement of the island is seen to either the right or left. Deintercalation then continues with further separation of the GEDs not associated with the island and the complete deintercalation of the guest island, as shown in Figure 11d,e. We have also observed similar guest–layer separation processes during the deintercalation of more internal guest layers.

The above deintercalation process provides direct support for the applicability of the Daumas–Hérold model to deintercalation reaction processes and staging phenomena.[26] According to this model, during the deintercalation of a stage-1 intercalate, entire guest layers do not simply deintercalate unidirectionally. Instead, they separate into islands during the deintercalation process, which deintercalate progressively. Thus, the observation of both guest–layer separation and island formation are consistent with the Daumas–Hérold model. Previous estimates of guest–island size range from 100 Å to macroscopic dimensions.[15,30,31] In

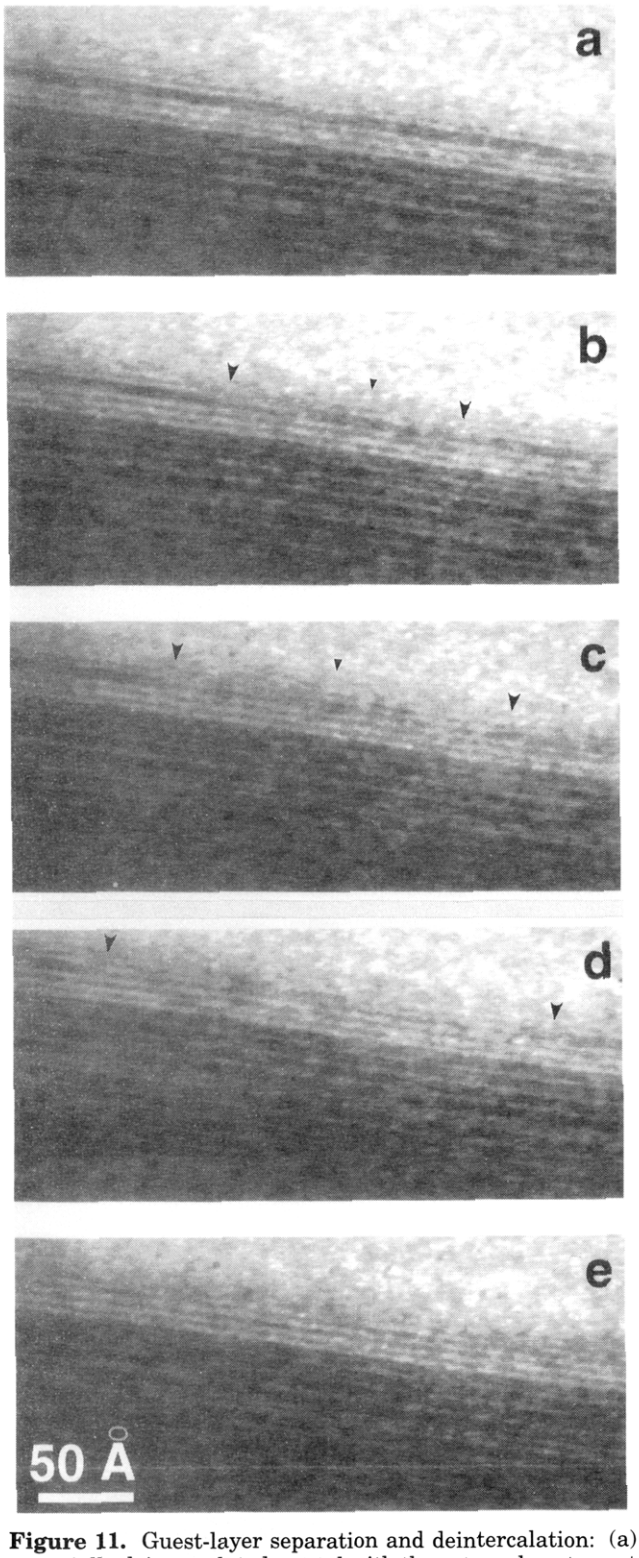

Figure 11. Guest-layer separation and deintercalation: (a) a partially deintercalated crystal with the externalmost guest layer fully intercalated; (b) this guest layer begins to separate in the middle into two GEDs and deintercalate, leaving an ≈70 Å guest island at the separation site; (c) the GEDs continue to migrate to the left and right, and the guest island shrinks to ≈40 Å across; (d) the island has completely deintercalated, and the GEDs have further separated; (e) the GEDs have deintercalated out of the field of view. The black arrows indicate the position of the GED terminations, and the black-on-white arrows indicate the position of the guest island.

this regard, it is important to note the guest−layer separation process shown in Figure 11 occurred in a crystal that was about 1000 Å wide (left to right) and 100 Å thick (parallel to the electron beam). Therefore, we do not expect to see the formation of many islands

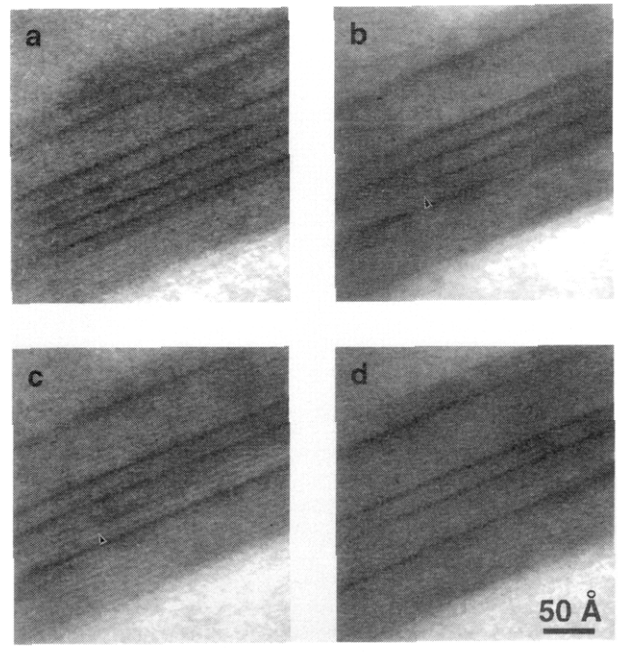

Figure 12. Guest−island separation from a deintercalating GED and their subsequent deintercalation: (a) a partially deintercalated crystal with four stage-3 packages in the middle of the intercalate; (b) the second-from-the-bottom guest layer in the stage-3 region begins to deintercalate to the right with the formation and movement of a GED; (c) a new GED separates from the old GED and deintercalates out of the field of view to the right, leaving behind a small guest island; (d) the small guest island has deintercalated parallel to the electron beam. The arrows in (b) and (c) indicate the position of the initial GED termination and the unchanged position of the end of the guest island, respectively.

in this crystal, or any crystal suitable for HRTEM observation, due to the small crystal dimensions, especially parallel to the electron beam.

The small island formed during guest−layer separation in Figure 11 indicates the separation of guest layers can involve the formation of intermediate guest islands. If such a guest island formed during guest−layer separation in the interior of a substantially larger crystallite, it could very likely become "trapped" by its domain-wall boundaries during deintercalation. Such a process could result in the formation of the so-called "residue" intercalation compounds, which retain small concentrations of guest species when complete deintercalation is difficult.[1-7]

2. GED Deintercalation and Island Formation. The formation of guest islands during the deintercalation process need not be associated exclusively with the guest−layer separation process. As shown in Figure 12, it can also be associated with the unidirectional deintercalation of a GED. Figure 12a shows four stage-3 packages in the middle of a region consisting primarily of host layers. The second guest layer from the bottom begins to deintercalate via GED motion to the right, as shown in Figure 12b. Then, after pausing for a few seconds in the position shown in Figure 12b, a small guest island forms as the result of the separation of a new GED that deintercalates to the right, as shown in Figure 12c. This island deintercalates parallel to the electron beam after several seconds, as seen in Figure 12d. We conclude that deintercalation occurred parallel to the electron beam because of the lack of island motion to either the left or right during deintercalation. As discussed above for the guest−layer separation process,

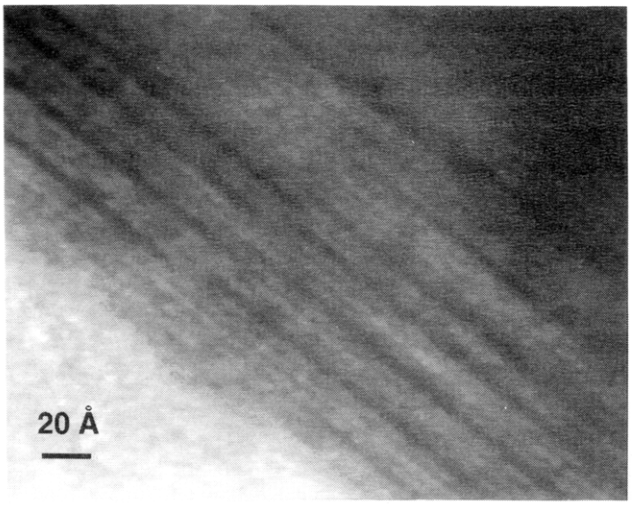

Figure 13. A more extensive staggered domain-wall boundary with opposing GEDs in adjacent guest layers and separated by a host layer.

if such a guest island were left behind during deintercalation in the interior of a substantially larger crystallite, it would probably become a "trapped" residual island in the crystal interior.[1-7]

3. GEDs: Formation of Stable Staggered Domain Walls. We often observed GED terminations forming staggered domain walls. The formation of these domain walls is fundamental to the formation of kinetically stable Daumas–Hérold guest–island domains predicted theoretically for intercalation/deintercalation reaction processes.[14-18] Models of guest–island/GED domains interacting via asymmetric and symmetric staggered domain walls are shown in Figure 2. Once formed, staggered domain walls were quite stable to further deintercalation. An example of their formation and stability is shown in Figure 9e,f, where two opposing GEDs begin to deintercalate in opposite directions in Figure 9e and continue to deintercalate until they form a stable staggered domain-wall pair shown in Figure 9f. This staggered domain-wall pair was quite stable, even though there is an additional host layer in between the GED-containing layers.

A more extensive staggered domain wall is shown in Figure 13, where both adjacent-layer GED terminations and GED terminations separated by a host layer have formed a stable staggered domain-wall structure. The formation of staggered domain-wall boundaries routinely inhibited further deintercalation, as predicted theoretically due to the attraction of guest islands in neighboring layers resulting in stable Daumas–Hérold domain formation.[14-17,26]

As shown in both Figures 9 and 13, the elastic stabilization of staggered domain walls is not restricted to nearest-neighbor guest layers and can extend to next-nearest-neighbor guest layers as well. Some elastic stability was observed for opposing GED terminations as far as several layers apart. The stabilization energy is expected to decrease with greater interlayer separation of the GED terminations. Stable domains were also observed for GEDs that deintercalated until their terminations came into close proximity of an oppositely directed HED termination in a nearby layer, as discussed previously, demonstrating the elastic nature of these interactions.

4. Symmetric and asymmetric GED terminations: Intercalation or deintercalation of a guest layer that involves restacking of the host layers requires host–layer slippage at the GED termination if both the intercalate and host domains are to retain their equilibrium stacking configurations. This can be accommodated by the formation of an asymmetric GED termination in which one host layer bends more than the other around the termination, as shown in Figure 2a.[15,16] For those intercalates that have the same stacking arrangement as their hosts, such slippage is not necessary. In this case, symmetric GED terminations are expected, as depicted in Figure 2b.[15,16]

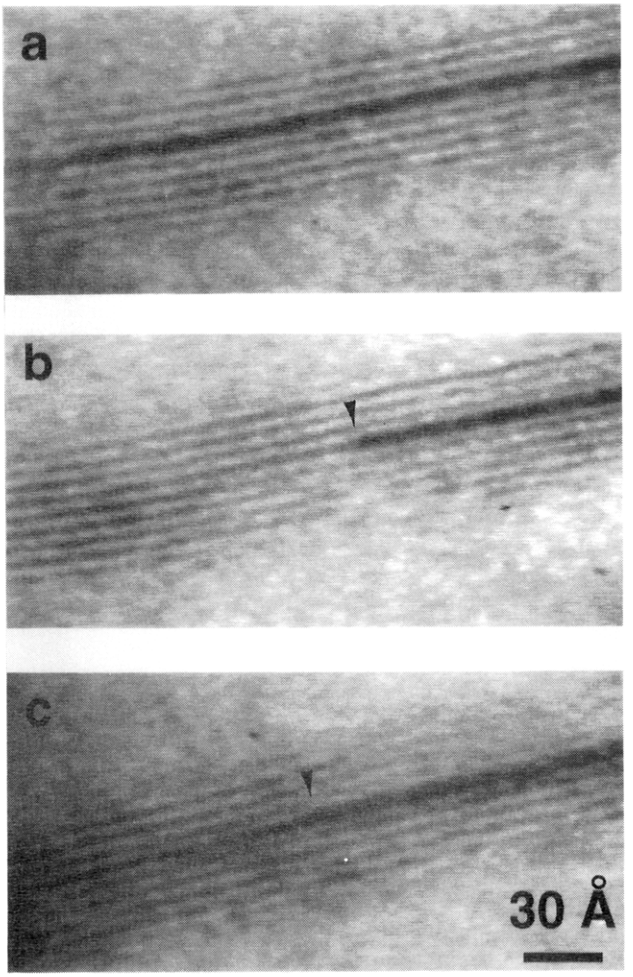

Figure 14. Transition from a symmetric to an asymmetric GED termination during guest–layer deintercalation: (a) the completely intercalated guest layer; (b) partial deintercalation of the layer to the right, with the formation of a symmetric GED termination; (c) continued deintercalation of the layer to the right, with the formation of an asymmetric GED termination a few hundred angstroms to the right of the position of the symmetric GED termination in (b). The arrows in (b) and (c) indicate the positions of the GED terminations.

Rietveld refinement of XPD data together with HR-TEM structural analysis indicates the TiS_2 host layers, which octahedrally coordinate the empty guest galleries, restack during Hg intercalation.[40,42,43] Therefore, equilibrium host–layer stacking on both the intercalated and deintercalated side of Hg_xTiS_2 GED terminations is expected to result in asymmetric terminations.[15,16]

In the course of this investigation, both symmetric and asymmetric GED terminations were observed. Figure 14 shows the progression of the GED termination structure during deintercalation. Figure 14a shows a fully intercalated guest layer. Deintercalation starts with the formation and left-to-right movement of a GED with a symmetric termination, as shown in Figure 14b,

Table 1. Internal-Layer Deintercalation Onset Associated with Surface and Internal Defects

location	defect type	description
surface	layer step	onset occurs at a guest layer situated between host layers that terminate in a step structure at the crystal edge
	irregular host-layer termination	onset occurs at guest layers whose neighboring host layers terminate irregularly at the crystal surface
internal	host–layer edge dislocation	onset occurs in the guest layers adjacent or near to a host–layer edge dislocation
	interlayer defect	onset occurs in the guest layer situated between misaligned host layers

despite the different sulfur stacking arrangements expected for TiS_2 and $Hg_{1.25}TiS_2$. However, further deintercalation eventually results in the formation of an asymmetric GED termination, as shown in Figure 14c.

The transition from a symmetric to an asymmetric GED termination can be related to a delayed restacking of the host–layer sulfur atoms about the gallery. At the onset of guest–layer deintercalation, the thermodynamic restacking energy is very small, since, to a first approximation, it is proportional to the area of the host–layer interface. Therefore, the initial stacking of the deintercalated region of the gallery can be influenced by the local structure surrounding the onset region, which may not favor restacking. As deintercalation continues to progress and the area of the deintercalated region of the guest gallery continues to grow, restacking becomes increasingly favorable energetically and eventually will occur, as shown in Figure 14c.

In contrast, the GED terminations initially formed in Figure 11 are asymmetric, consistent with rapid host–layer restacking. This highlights another factor that contributes to the formation of asymmetric, instead of symmetric, GED terminations, which is the minimization of the elastic strain in the region surrounding the GED termination. Crystals whose GED terminations are surrounded by very few additional layers on one side and substantially more on the other, i.e., near-surface GED terminations, were generally observed to form asymmetric terminations, as shown in Figure 11. By forming asymmetric GED terminations near the external basal plane, the strain transmitted to the neighboring layers by the GED termination can be reduced. This reduction is accomplished by limiting the number of elastically strained neighboring layers to a small number of surface layers instead of the more abundant interior layers. It is possible that such a near-surface process may occur early during guest–layer deintercalation, even if restacking is not otherwise thermodynamically favorable.

It is important to note that the symmetric GED termination observed in Figure 14b has similar numbers of host layers on either side (4 and 5) to which the GED termination strain is distributed, so that no substantial strain relief would be gained by initially forming an asymmetric GED termination. However, once the restacking energy has increased due to further deintercalation and the GED termination transforms to asymmetric, it bends to the side that strains the least number of neighboring layers, as depicted in Figure 14c.

Staggered domain walls were most often observed to be asymmetric in nature, resulting from the interaction of asymmetric GED terminations, as shown for two opposing GEDs with an interleaving host layer in Figure 9f. The staggered domain wall in Figure 13 also appears to have primarily asymmetric character, although the exact domain-wall structure is not well resolved. Similar asymmetric walls have been predicted for intercalation systems that experience host–layer restacking.[15,16] In addition to accomodating host–layer restacking, such asymmetric pairing of opposing GEDs also has the advantage of being able to confine nearby layer strain to the layer(s) between the GED pair, as shown in Figure 2a.

As shown in Figures 9f and 13, the *c* axis offsets of the host layers across the staggered domain walls are small, which minimizes their host-layer elastic strain energy. Large *c* axis offsets of host layers across the domain walls were not observed.[15,16,48]

Conclusions

DHRTEM has provided the first detailed atomic-level images of the onset and progression of deintercalation processes, including the observation of staging and individual guest and host–layer behavior, for the model neutral intercalate Hg_xTiS_2 ($1.25 \geq x > 0.00$). The onset of the deintercalation process was most often observed to occur at the outermost guest layers adjacent to the most flexible host layers. However, the onset of deintercalation was also frequently observed to occur at internal guest layers. In the latter case, the internal layers exhibiting enhanced deintercalation reactivity can be correlated with various surface and internal lattice defects that lower their deintercalation activation energy, as summarized in Table 1. Such defects can play major roles in the Hg_xTiS_2 deintercalation process, dictating both the onset layers and the general progression of deintercalation.

Once started in either outermost or internal guest layers, deintercalation primarily proceeds by the sequential deintercalation of guest layers progressively further away from the onset layer(s). Seldom do neighboring layers repetitively deintercalate in succession. Instead, stage-disordered, primarily randomly staged, intercalate regions form and expand away from the onset layer(s), with the concurrent deintercalation of some guest layers within the regions. Local stage-ordered repeats are occasionally formed in the process. Overall, the deintercalation process, in the presence or absence of defects, is best described as a nucleation and growth process. The process nucleates at the onset layers, after which primarily randomly staged regions grow away from these layers.

The progression of deintercalation away from internal, in addition to outermost, onset layers can have a substantial affect on sample inhomogeneity during deintercalation. For instance, if deintercalation solely progresses inward from the basal planes of a relatively large crystallite, the sample should be inhomogeneous during the deintercalation process, with two reaction fronts moving toward the inner layers. Such a process is analogous to the intercalation process proposed by Hooley, in which intercalation starts at the outermost

(48) Ulloa, S. E.; Kirczenow, G. *Phys. Rev. B* **1986**, *33*, 1360.

lamellar regions associated with adsorbate-host charge transfer and/or the enhanced flexibility of the external host layers.[36,37] However, larger crystallites also likely contain more defects which can initiate internal onset. Consequently, it appears deintercalation can generally progress away from multiple onset layers for larger crystallites, resulting in a much lower level of inhomogeneity during deintercalation transitions. Whether or not internal onset may apply to intercalation processes as well is currently under investigation in our laboratories. Such studies should provide insight into the relationship between sample inhomogeneities and the continuity of intercalation staging transitions.[23,25]

Our DHRTEM observations provide direct support for the formation and deintercalation of guest islands being an integral part of the deintercalation process. First, the formation of small guest islands ($\lesssim$100 Å) was generally observed during the course of deintercalation. The intercalate crystals observed were unable to support larger islands due to their small dimensions. Second, guest–layer separation was routinely observed for completely filled layers, with the GEDs formed deintercalating in opposite directions, consistent with the separation of guest layers into islands during bulk deintercalation processes. Third, small guest islands were observed to separate from GEDs during deintercalation. Fourth, the formation of kinetically very stable GED-termination staggered domain-wall boundaries was routinely observed.

The behavior of GED-termination staggered domain-wall boundaries during these investigations can help elucidate the interactions that occur at the similar staggered domain-wall boundaries expected for guest–island interactions.[14-18] Such staggered domains were routinely observed to form with relatively strong binding interactions in the course of these studies, providing direct experimental support for Kirczenow's theoretical prediction that guest–island staggered domains should bind together in GICs.[49] The interlayer range of these interactions can extend beyond neighboring staggered GED terminations, since at least some binding interaction was observed for opposing terminations separated by up to several host layers. The binding interactions for staggered domains are in sharp contrast to the relatively large energy barriers predicted by Kirczenow to separate matching guest domains, i.e., guest domains in the same gallery.[49] Such barriers are consistent with the observations herein and may explain why once guest islands/edge dislocations formed during deintercalation they were never observed to merge. However, DHRTEM observations of intercalation processes should provide better insight into the presence of such barriers, as guest domain growth is not inherently associated with deintercalation. The binding of staggered domains and the energy barriers separating matching domains can be directly associated with the stability of guest islands and relatively slow reaction kinetics often associated with TMD and graphite intercalation/deintercalation processes.

The formation of asymmetric, as opposed to symmetric, GED terminations during deintercalation is associated with host–layer restacking across the termination. Their formation has also been observed to be dependent, at least kinetically, on the proximity of the GED to an externalmost host layer and the area of the empty guest gallery left behind by deintercalation. Although internal guest layers can form symmetric GED terminations initially, as deintercalation continues, host–layer restacking is increasingly favorable energetically and eventually leads to the formation of asymmetric GED terminations. Near-surface GED terminations, in contrast, generally form asymmetric terminations initially to minimize the number of intercalate layers that are strained by the termination.

Acknowledgment. We wish to acknowledge the National Science Foundation for support through Grant DMR 91-06792, and acknowledgment is made to the donors of the Petroleum Research Fund, administered by the American Chemical Society, for partial support of this research. We also wish to thank the Center for Solid State Science for use of its Materials Science Electron Microscope Laboratory and Materials Preparation Facility.

(49) Kirczenow, G. *Phys. Rev. Lett.* **1982**, *49*, 1853.